Pharmaceutical Development and Technology

ISSN: (Print) (Online) Journal homepage: https://www.tandfonline.com/loi/iphd20

# Spray drying of naproxen and naproxen sodium for improved tableting and dissolution – physicochemical characterization and compression performance

Nizar Al-Zoubi , Faten Odeh , Ioannis Partheniadis , Shadi Gharaibeh & Ioannis Nikolakakis

**To cite this article:** Nizar Al-Zoubi , Faten Odeh , Ioannis Partheniadis , Shadi Gharaibeh & Ioannis Nikolakakis (2021) Spray drying of naproxen and naproxen sodium for improved tableting and dissolution – physicochemical characterization and compression performance, Pharmaceutical Development and Technology, 26:2, 193-208, DOI: 10.1080/10837450.2020.1853769

**To link to this article:** https://doi.org/10.1080/10837450.2020.1853769

PHARMACEUTICAL DEVELOPMENT AND TECHNOLOGY
2021, VOL. 26, NO. 2, 193–208
https://doi.org/10.1080/10837450.2020.1853769

Taylor & Francis
Taylor & Francis Group

RESEARCH ARTICLE



# Spray drying of naproxen and naproxen sodium for improved tableting and dissolution – physicochemical characterization and compression performance

Nizar Al-Zoubi[a], Faten Odeh[b], Ioannis Partheniadis[c], Shadi Gharaibeh[d] and Ioannis Nikolakakis[c]

[a]Department of Pharmaceutics and Pharmaceutical Technology, Faculty of Pharmaceutical Sciences, The Hashemite University, Zarqa, Jordan; [b]Department of Pharmaceutical Sciences and Pharmaceutics, Faculty of Pharmacy, Applied Science Private University, Amman, Jordan; [c]Department of Pharmaceutical Technology, School of Pharmacy, Faculty of Health Sciences, Aristotle University of Thessaloniki, Thessaloniki, Greece; [d]Faculty of Pharmacy, Jerash University, Jerash, Jordan

**ABSTRACT**

In this work, the tabletability and dissolution of spray-dried forms of naproxen and its sodium salt were compared with those of unprocessed drugs. Solutions of naproxen or naproxen sodium alone or with HPMC (5% w/w of drug content) were spray dried. Scanning electron micrographs showed that naproxen sodium spray-dried particles were spherical, whereas those of naproxen were non-spherical but isodiametric. Powder x-ray diffraction and thermal analysis indicated that co-spray drying with HPMC resulted in reduced crystallinity of naproxen and higher naproxen sodium dihydrate content. FTIR and Raman analysis showed shifting, merging or elimination of bands in the spectra of the co-spray dried products signifying solid-state alterations. When mixed with suitable processing aids (7% w/w), all co-spray dried powders produced satisfactory tablets in the pressure range 73–295 MPa. Conversely, physical mixtures of naproxen compressed with the same aids failed tableting, whereas naproxen sodium produced weak tablets. Dissolution tests showed significant improvement for co-spray dried drugs tablets. Therefore, since the large therapeutic doses of naproxen and sodium naproxen limit the use of tableting aids, the improved compaction and dissolution performance of the spray-dried forms may be a formulation alternative.

**ARTICLE HISTORY**
Received 9 May 2020
Revised 16 November 2020
Accepted 17 November 2020

**KEYWORDS**
Spray drying; compaction; solid-state; tableting; differential scanning calorimetry (DSC); thermogravimetric analysis (TGA); infrared (IR) spectroscopy; Raman spectroscopy; powder x-ray diffraction (PXRD)

## 1. Introduction

Tableting by direct compression is one of the simplest and most cost-effective approaches for drug manufacturing. However, for most high-dose active pharmaceutical ingredients (APIs), the applicability of direct compression is limited due to suboptimal powder flowability, compressibility and compactability. To overcome these limitations, many API manufacturing companies attempt to develop direct compression grades of high-dose APIs.

Naproxen is an over-the-counter nonsteroidal anti-inflammatory drug (NSAID) of low COX-2 selectivity resulting in lower cardiovascular risk than other NSAIDs (Angiolillo and Weisman 2017). It is manufactured and marketed as the weakly acidic compound (e.g. Naprosyn®) or as the sodium salt (e.g. Naprelan®). Naproxen is an odorless white to off-white crystalline substance. It is practically insoluble in water at low pH but freely soluble at high pH. Naproxen sodium is a white to creamy white crystalline solid, freely soluble in water at neutral pH. Tableting of naproxen by direct compression is problematic due to the poor compressibility associated with its relatively high dose (from 250 to 500 mg) (Maghsoodi et al. 2008, 2007). Similarly, naproxen sodium is given in large-dose tablets (from 275 to 550 mg) and is normally processed by wet granulation to improve tableting behavior (Di Martino et al. 2008). For such high-dose drugs, to overcome the extra cost and granulation time, many pharmaceutical manufacturers prefer to use directly compressible grades of active ingredients provided that the resulting tablets have acceptable mechanical strength and dissolution profile.

There have been some attempts to enhance the compactability of naproxen and its sodium salt. Maghsoodi et al. (2007) used spherical crystallization in the presence of various concentrations of hydroxypropyl cellulose (HPC) to obtain spheroidal particles and reported enhanced flow and compression. The work was extended and crystallo-co-agglomeration was applied to include the superdisintegrant sodium starch glycolate in the spherical agglomerates (Maghsoodi et al. 2008). The compression behavior of naproxen sodium has also been evaluated for anhydrous and hydrate forms (Joiris et al. 2008; Malaj et al. 2010) and for wet granules obtained by high shear granulation (Di Martino et al. 2008). The results demonstrated improved deformability due to the increased hydration level, which might be controlled by the drying method (Di Martino et al. 2008).

Spray drying is a continuous particle engineering process used in the pharmaceutical industry to produce fine or agglomerated powders with a narrow size range and spherical particles. Its main advantage is the capability to co-process two or more materials into composite particles in order to manipulate dissolution and/or improve tableting properties. Accordingly, it is used in the preparation of many commercially available direct compression excipients. Several researchers have used spray drying to improve the compression of APIs that require large administration doses such as acetazolamide (Di Martino et al. 2001), acetaminophen,

CONTACT Nizar Al-Zoubi nzoubi@hu.edu.jo Department of Pharmaceutics and Pharmaceutical Technology, Faculty of Pharmaceutical Sciences, The Hashemite University, Zarqa, 13115, Jordan; Ioannis Nikolakakis yannikos@pharm.auth.gr Department of Pharmaceutical Technology, School of Pharmacy, Faculty of Health Sciences, Aristotle University of Thessaloniki, Thessaloniki, 54124, Greece

ibuprofen and cimetidine (Gonnissen et al. 2007; 2008), chlorothiazide and its salts (Paluch et al. 2012, 2013), celecoxib (Joshi et al. 2010), metformin HCl (Barot et al. 2010; Al-Zoubi et al. 2017) and cefuroxime axetil (Rathod et al. 2019). Although spray drying of naproxen or naproxen sodium has been investigated, so far, the studies have been focused on the characteristics of the produced solid dispersion (Maheri-Esfanjani et al. 2012; Paudel and Van Den Mooter 2012; Paudel et al. 2013; Worku et al. 2014) and drug release control (Arici et al. 2014) without addressing the issue of compression.

Therefore, the objectives of this work were first to study the effects of spray drying on the solid-state properties of naproxen and naproxen sodium by characterizing the products using SEM, PXRD, thermal analysis and vibration spectroscopy. Then, to see if changes occurring in the solid state are realized in the compression behavior and dissolution, possibly resulting in better tablet quality.

## 2. Materials and methods

### 2.1. Materials

The following materials were kindly donated: naproxen by JPM (Amman, Jordan), naproxen sodium by Ram Pharma (Amman, Jordan), hypromellose (HPMC, Benecel™ E3 Pharm) by Ashland, crospovidone (Kollidon® CL) by BASF (Ludwigshafen, Germany) and sodium stearyl fumarate (Pruv®) by JRS Pharma GmbH & Co. KG (Rosenberg, Germany). Talc was purchased from Liaoning Jiayi metals & minerals co. Ltd (Dalian, China).

### 2.2. Preparation of spray-dried powders

Spray drying was carried out in a Pulvis mini-spray GA 32 (Yamato Scientific, Japan) equipped with a 406 μm two-fluid nozzle. The sodium salt of naproxen is freely soluble in water, whereas the free acid is practically insoluble (British Pharmacopeia Commission 2020). Therefore, naproxen was dissolved in 80% v/v isopropanol/water solvent system (solubility at 30 °C = 3.8% w/v, Mohammadzade et al. 2015) or HPMC solution in the same solvent. The total solids concentration was kept constant (3.5% w/v). Spray drying was applied under the following conditions: inlet air temperature 100 °C, outlet air temperature 60–62 °C, air pressure 1 kg/cm$^2$, feed rate 25 ml/min. Naproxen sodium was dissolved in distilled water or aqueous HPMC solution. The total solids concentration was kept constant (16% w/v). The resulting solution was spray dried under the following conditions: inlet air temperature 120 °C, outlet air temperature 78–82 °C, air pressure 1 kg/cm$^2$, feed rate 11 ml/min. The experimental batches of naproxen and naproxen sodium unprocessed, spray-dried and co-spray dried batches are given in Table 1 together with batch codes.

The spray-dried powders collected at the receiving vessel were accurately weighed and from the weight, the production yield was expressed as percentage of the total initial solids content in the spray-dried solution. Powders were kept in tightly closed plastic containers and stored in a desiccator over silica gel for examination.

Table 1. Batch codes and experimental naproxen and naproxen sodium batches.

| Batch codes | Drug | Processing | HPMC (w/w %) |
|---|---|---|---|
| N-RM | naproxen | None | 0 |
| N-SD | naproxen | Spray drying | 0 |
| N-CSD | naproxen | Co-spray drying | 5 |
| NS-RM | Sodium naproxen | None | 0 |
| NS-SD | Sodium naproxen | Spray drying | 0 |
| NS-CSD | Sodium naproxen | Co-spray drying | 5 |

### 2.3. Characterization of spray-dried powders

#### 2.3.1. Particle size

Median particle size and particle size distribution (expressed as $X_{90}/X_{10}$) were estimated utilizing two techniques: (i) laser diffraction particle size analyzer equipped with a dry powder accessory (Mastersizer 2000 A, Malvern, UK) and (ii) optical microscopy with image analysis system using an Olympus BX41 microscope fitted with upper single port and camera image adapter extensions (U-SPT and U-PMTVC, Olympus Corporation, Tokyo, Japan), Leica DF295 video camera (Leica, Germany) and Leica Microsystems software (Leica, Switzerland). About 300 particles dispersed in paraffin oil were analysed in different fields. Particle size was expressed as projected equivalent circle area diameter.

#### 2.3.2. Field emission gun scanning electron microscopy (FEG-SEM)

Morphology of the spray-dried products and the raw materials of naproxen and naproxen sodium was examined by FEG-SEM (FEI Company – FEI Quanta 450 FEG, Eindhoven, Netherlands). Samples were coated with 1.5 nm of gold in a sputter coater (Emitech K550X, UK) and analyzed at 3.00 kV and 2500× magnification.

#### 2.3.3. Particle density

Particle density was determined using helium pycnometry (Ultrapycnometer 1000, Quantachrome Instruments, Boynton) by measuring the volume of accurately weighted samples (average of 10 runs). The instrument was calibrated with a standard 7.0699 cm$^3$ steel ball.

#### 2.3.4. Simultaneous thermal analysis

Simultaneous thermogravimetric analysis (TGA) and differential scanning calorimetry (DSC) of unprocessed, spray-dried and co-spray dried products were examined using a Netzsch STA 409 PC (Germany). Samples (~3 mg) were weighed and placed in perforated aluminum pans. The samples were heated under nitrogen atmosphere at a rate of 10 °C/min from ambient temperature to 200 °C or 280 °C for naproxen and naproxen sodium, respectively. The water content of samples was calculated based on the weight loss (%) recorded between 50 and 150 °C.

#### 2.3.5. Powder x-ray diffraction (PXRD)

For the characterization of the crystallinity of the unprocessed drugs and spray-dried products, PXRD patterns were recorded at room temperature (25 °C) using a Rigaku Ultima IV diffractometer (Japan) fitted with a Cu anode operated at 40 kV and 40 mA. The cavity of the specimen holder of the diffractometer was filled with sample powder and then smoothed out with a spatula. Samples were scanned at a rate of 4° min$^{-1}$ from 5 to 60° 2$\theta$.

#### 2.3.6. Vibration spectroscopy

*FTIR and Raman* spectroscopic analyses of unprocessed, spray-dried and co-spray dried drugs were performed to detect changes in the spectra of the two naproxen forms due to spray drying. FTIR spectra were obtained using Attenuated Reflectance Fourier Transform Infrared Spectroscopy (ATR-FTIR) (Prestige-21, Shimadzu, Kyoto, Japan). The FTIR spectrometer was attached to a horizontal Golden Gate MKII single-reflection ATR system (Specac, Kent, UK) equipped with a Diamond/ZnSe crystal (45° angle to infrared beam, 1.66 μm at 1000/cm depth of penetration, 2.4

refractive index and 525/cm long wavelength cut-off). Spectra were acquired in transmission mode in the range 4000–650 $cm^{-1}$ as an average of 64 cumulative spectra at 4 $cm^{-1}$ resolution.

Raman spectra were obtained using a Raman spectrometer (Agility-2TM, BaySpec Inc., CA). A small powder sample was placed in a standard glass vial and measured at 785 nm laser excitation line. Resolution was 12 $cm^{-1}$, exposure time 5 s, power of the incident laser beam 250 mW and the recorded spectra were average of 75 runs. Origin pro 9 software (OriginLab Corporation, MA) was used for processing of the spectra.

Additionally, FTIR spectra of co-spray dried naproxen sodium compressed tablets were taken to check if there is any solid-state transformation of the hydrate to anhydrous drug during compression. The tablets were first crushed into powder in an agate mortar (O.D. 65 mm; Sigma-Aldrich, St. Louis, MO) and the size fraction <125 μm (close to the size range of uncompressed powders) was separated for analysis.

### 2.4. Preparation of ready-to-compress (RTC) mixtures of naproxen and naproxen sodium with processing aids

Unprocessed and spray-dried powders were placed in glass bottles with 5% w/w crospovidone (as disintegrant and dry binder) and blended in a Turbula mixer (Bachofen, Switzerland) for 10 min. Then, 1% w/w sodium stearyl fumarate and 1% w/w talc were added for lubrication and flow improvement and further mixed for 5 min.

### 2.5. Force-displacement profiles

Force-displacement (f/d) profiles of RTC mixtures were recorded using an instrumented benchtop tablet press (Model GTP-1, Gamlen Tableting Ltd, Nottingham, UK) fitted with 6-mm flat-faced punches. It was operated at 60 mm/min speed and 174 MPa maximum compression pressure. RTC powder mixtures (100 mg) were introduced into the die and f/d profiles were recorded during compression, decompression and ejection.

The area under the recorded f/d compression curve (Figure 1) was used to estimate the work of compression, $W_c$ (plastic energy, PE) and the area confined between the recorded curve and the line drawn perpendicular to the point of maximum applied force was used to estimate the work of decompression, $W_d$ (elastic energy, EE). The elastic/plastic energy ratio (EE/PE) was used as an index of the relative energy expended during decompression (Garekani et al. 2001). In addition, the deformation behavior of compacted powders was examined using derivative compression curves as previously described (Gharaibeh and Aburub 2013). The maximum force during tablet ejection ($F_{ej}$) was also recorded and was used as an estimate of compact friction and adhesion to the die wall (Al-Zoubi et al. 2016).

### 2.6. Tablet tensile strength

Samples (500 mg) of RTC mixtures were compressed for 30 s in a 13-mm diameter die and flat-faced punches set, employing a manually operated hydraulic press (Riken Seiki, Japan) at different pressures. 24-h after compression, the diameter and thickness were measured using a digital caliper (accuracy 0.01 mm). The force required to break the tablets was measured using an Erweka TBH 325 hardness tester (Erweka GmbH, Heusenstamm, Germany). Tensile strength was calculated according to Fell and Newton (1970):

$$\text{Tensile strength} = \frac{2 \times P}{\pi \times D \times t} \quad (1)$$

P is the fracture force and D and t are the diameter and thickness of the tablet, respectively.

### 2.7. In-vitro dissolution

*In-vitro* release of naproxen and sodium naproxen unprocessed, spray dried and co-spray dried tablets was tested using the USP II Apparatus at 100 rpm rotation paddle speed and 37 ± 0.5 °C for 2 h. Tablets of naproxen or naproxen sodium were added into 900 ml dissolution fluid. Since naproxen is insoluble in acidic pH, the tests were conducted in simulated intestinal fluid (pH 6.8). The pH was checked at the beginning and at the end of the test to ensure constancy. Aliquots were taken at timely intervals and analysed by UV spectroscopy (Pharma Spec UV-1700 Shimadzu, Kyoto, Japan) at 271.4 nm where clear peak was recorded (Figure 2). The reference curves at pH 6.8 are expressed with Equations (1) for naproxen and (2) for naproxen sodium with linearity in the range of 3.5–12.7 μg/mL ($R^2$ = 0.999) and 2.8–15.8 μg/mL ($R^2$ = 0.999), respectively.

$$C\ (\mu g/mL) = (Abs + 0.0901)/0.0292) \quad (1)$$

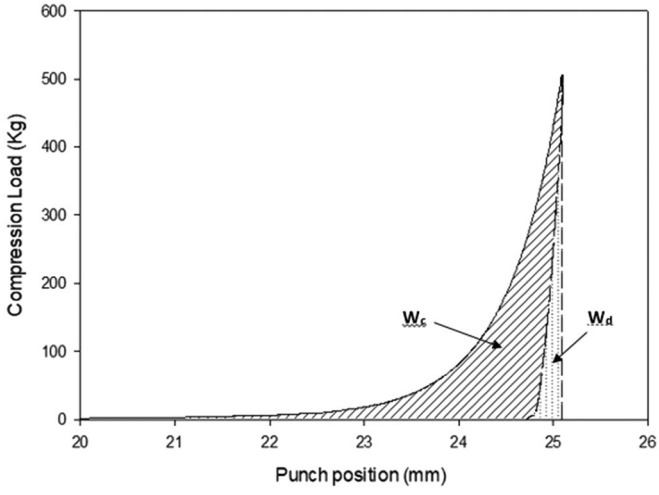


Figure 1. Force-displacement profile showing the areas corresponding to work of compaction ($W_c$) and work of decompression ($W_d$).

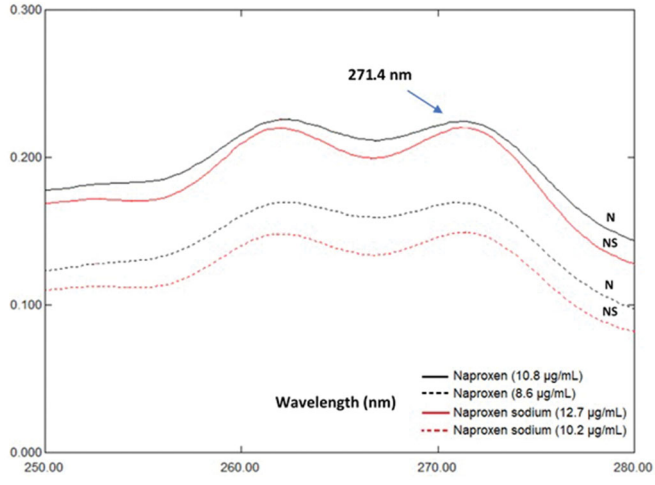


Figure 2. UV spectra of naproxen (N) and naproxen sodium (NS).

$$C\ (\mu g/mL) = (Abs + 0.0457)/0.0194) \quad (2)$$

Drug release was expressed as % of nominal content and 85% release after 15 min was considered as instant release (FDA 1997).

In addition, the overall dissolution profiles obtained from the tablets prepared by the spray-dried alone or co-spray dried drugs was compared with that of the tablets of unprocessed drugs using the similarity factor ($f_2$), details of which are given elsewhere (Sanoufi et al. 2020). Finally, the %drug released after 15 min was recorded and used to compare the 'instant' release performance.

### 2.8. Accelerated stability test

Dissolution profiles and tablet strength were also tested for tablets that were exposed for one week to relative humidity of 75% (desiccator with saturated NaCl solution) at 40 °C. The results of the accelerated test were compared with those on tablets kept at ambient conditions (RH% ~ 40 and temperature ~ 20 °C.

## 3. Results and discussion

### 3.1. Production yield, particle size and water content

Experimental batches and codes are presented in Table 1. Naproxen and naproxen sodium were the two forms of the drug, examined as unprocessed (N-RM and NS-RM, respectively), spray-dried (N-SD and NS-SD) and co-spray dried (N-CSD and NS-CSD) powders. Results of production yield, moisture content and particle size distribution (median and $X_{90}/X_{10}$) are shown in Table 2.

Production yield values ranged from 46.3 to 67.2% indicating suitable spray drying conditions. The values of median diameters measured by laser diffraction were between 7.6 and 24.5 μm and median diameters measured by microscopy were between 7.8 and 20.2 μm. Since the two methods of particle size analysis implement different principles for powder dispersion, shearing action in air current and dispersant liquid, respectively, the closeness of the diameter ranges indicates structural rigidity, and hence easy and safe handling. The spread of the particle size distribution ($X_{90}/X_{10}$) was also similar for both methods ($X_{90}/X_{10} \leq$ 20.9 and $\leq$17.8 for diffraction and microscopy, respectively). Naproxen and sodium naproxen batches prepared by co-spray drying with HPMC (N-CSD and NS-CSD, respectively) showed higher yield and median particle size than the corresponding spray-dried batches without polymer (N-SD and N-CSD, respectively). This is explained by the increased viscosity of the sprayed solution containing dissolved polymer. Higher solution viscosity produces larger particles and smaller amount of fines that are easily lost through the aspirator.

Table 2. Production yield, water content (WC%), particle size distribution parameters and particle density for naproxen and naproxen sodium unprocessed, spray-dried and co-spray dried powders with HPMC (batch codes as in Table 1).

| Batch code | Yield (%) | WC (%) | Particle size distribution | | | | Particle density (g/cm$^3$) |
|---|---|---|---|---|---|---|---|
| | | | Laser scattering | | Microscopy | | |
| | | | $X_{50}$ | $X_{90}/X_{10}$ | $X_{50}$ | $X_{90}/X_{10}$ | |
| N-RM | – | 0.5 | 24.5 | 10.2 | 20.2 | 7.2 | 1.298 |
| N-SD | 62.5 | 1.4 | 11.8 | 12.3 | 8.5 | 17.8 | 1.253 |
| N-CSD | 67.2 | 2.3 | 14.3 | 20.9 | 8.4 | 17.3 | 1.236 |
| NS-RM | – | 2.9 | 21.2 | 12.1 | 16.9 | 4.6 | 1.348 |
| NS-SD | 46.3 | 2.8 | 7.6 | 5.2 | 7.8 | 6.8 | 1.379 |
| NS-CSD | 57.5 | 5.4 | 15.2 | 10.3 | 11.7 | 6.5 | 1.355 |

Unprocessed naproxen (N-RM) and spray dried drug alone (N-SD) had lowest water contents of 1.6 and 0.5% due to the hydrophobic nature of the drug (Stubberud 1995). The slightly higher water content (2.3%) of the co-spray dried drug (N-CSD) should be attributed to the presence of the hydrophilic binder HPMC (Bhise et al., 2008).

The naproxen sodium forms showed higher water contents than naproxen forms due to the presence of the sodium ion and its potential to interact with water (Morris 1999). The water contents for unprocessed and spray dried alone salt were 2.9% and 2.8%, respectively, but for the co-spray dried form it was considerably higher (5.4%). The greater water content of co-spray dried naproxen sodium (5.4%) compared to the unprocessed or spray-dried alone (2.8, 2.9%) can be attributed to the higher viscosity of the spray-dried solution with dissolved polymer. The viscosity is expected to increase even more as drying progresses due to the increasing concentration of dissolved solids, resulting in lower evaporation rate and higher water content of the particles. Crystallization from aqueous solutions has been reported to yield a dihydrate (Di Martino et al. 2001; Kim and Rousseau 2004). However, since the theoretical water content in the monohydrate and dihydrate forms are 6.8% and 12.5%, respectively, and since there are reports that both the monohydrate and dihydrate are stable hydrates (Kim and Rousseau 2004; Censi et al. 2015), the co-spray dried products are probably mixtures of anhydrous with these two hydrates. This question was further examined by thermal, PXRD and spectroscopic analysis, as discussed later.

### 3.2. Scanning electron microscopy

Scanning electron micrographs (SEM) were acquired to examine the morphology and the extent of agglomeration of the spray-dried particles compared to the unprocessed. SEMs of unprocessed, spray-dried and co-spray dried powders with HPMC are shown in Figure 3. Naproxen (N-RM) was composed of large flaky particles, whereas naproxen sodium (NS-RM) was a mixture of large prismatic crystals and spherical particles. Application of spray or co-spray drying produced particle agglomerates, which for naproxen (N-SD, N-CSD) appear to be mixtures of spherical and irregular agglomerated particles, but for naproxen sodium (NS-SD, NS-CSD) were mostly spherical. The improved sphericity and the rigidity (see the previous section) of the spray-dried particles are good product attributes facilitating subsequent handling processes of the powder such as packing, flow, mixing and fluidization. Conversely, the irregularly shaped particles of the unprocessed naproxen and its sodium salt are expected to present problems due to the increased powder cohesiveness (Nikolakakis and Pilpel 1985).

### 3.3. Thermal analysis

In Figure 4, results of thermogravimetric analysis (TGA, Figure 4(a)) and differential scanning calorimetry analysis (Figure 4(b)) are shown for unprocessed, spray-dried and co-spray dried naproxen, whereas in Figure 5 are shown TGA recorded and derivatised curves for naproxen sodium. Results of differential scanning calorimetric analysis for the naproxen sodium forms are shown in Figure 6. Overall, the thermograms of naproxen sodium forms were more eventful than naproxen parent drug and for this reason they are discussed separately.

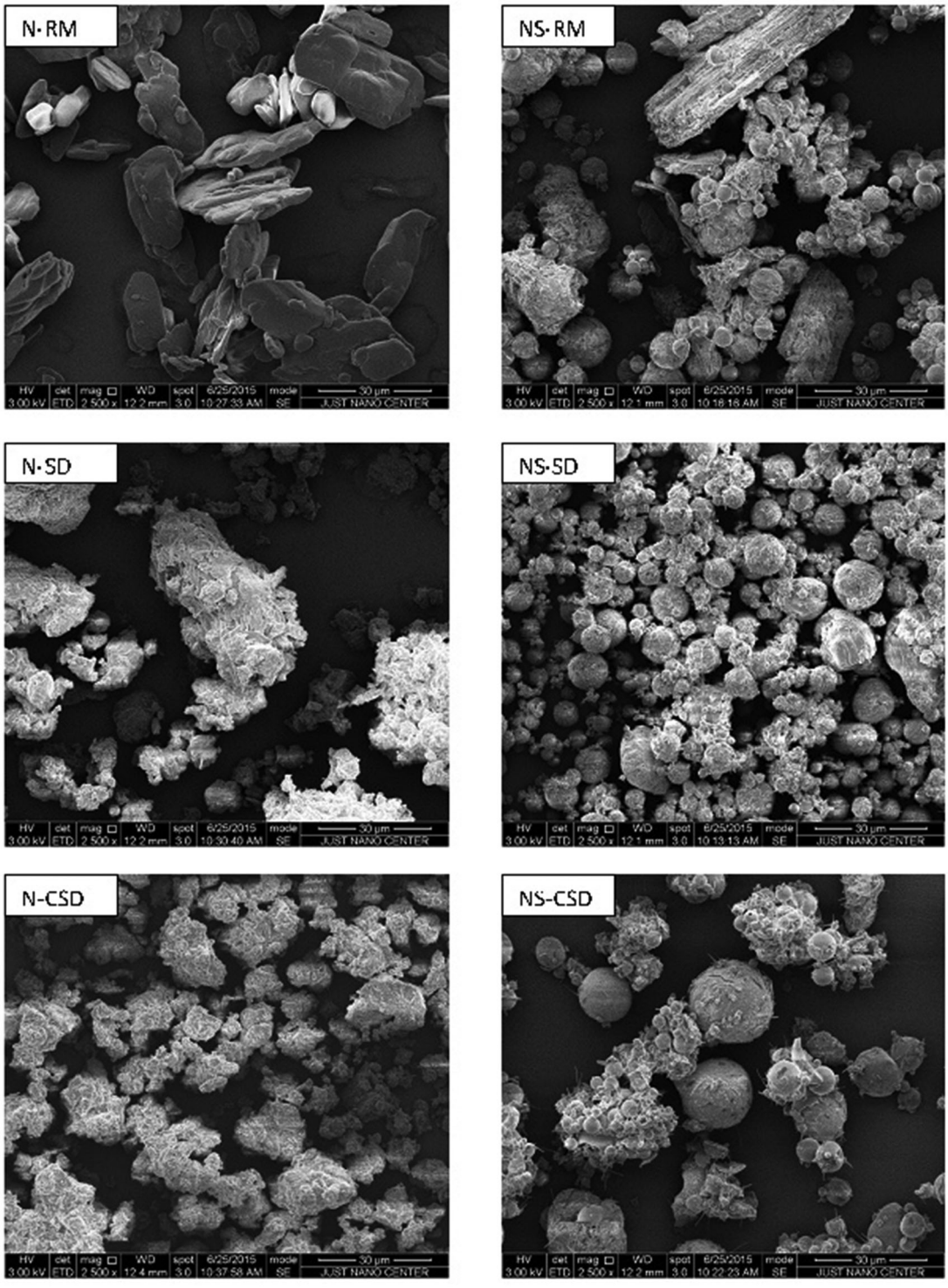


Figure 3. SEM micrographs for naproxen (unprocessed, N-RM; spray-dried N-SD; co-spray dried N-CSD) and naproxen sodium (unprocessed NS-RM; spray-dried NS-SD; co-spray dried NS-CSD).

### *3.3.1. Naproxen*

TGA: From the TGA plots (Figure 4(a)), it can be seen that the weight loss follows a nearly straight line decrease up with temperature up to about 160 °C. The decline is smaller for the unprocessed form (N-RM) compared to the spray-dried forms (N-SD, N-CSD), reflected in lower water content values (0.5% compared to 1.4% and 2.3%, Table 2).

DSC: From the three DSC thermograms (Figure 4(b)), it can be seen that each naproxen batch showed one clear endothermic peak corresponding to melting points of 163.3 °C for N-RM, 161.9 °C for N-SD and 161.0 °C for N-CSD. The corresponding melting enthalpies were 143.2, 122.2 and 100.5 μVs/mg, respectively. In the case of N-SD, the decrease of the m.p. can be attributed to lattice disruption to the fast molecule rearrangement during spray drying, as indicated by the PXRD results explained later. In the case of N-CSD where the drop is greater, the depression of the m.p. should be attributed to the interaction between the drug and the polymer resulting in relaxation of the lattice

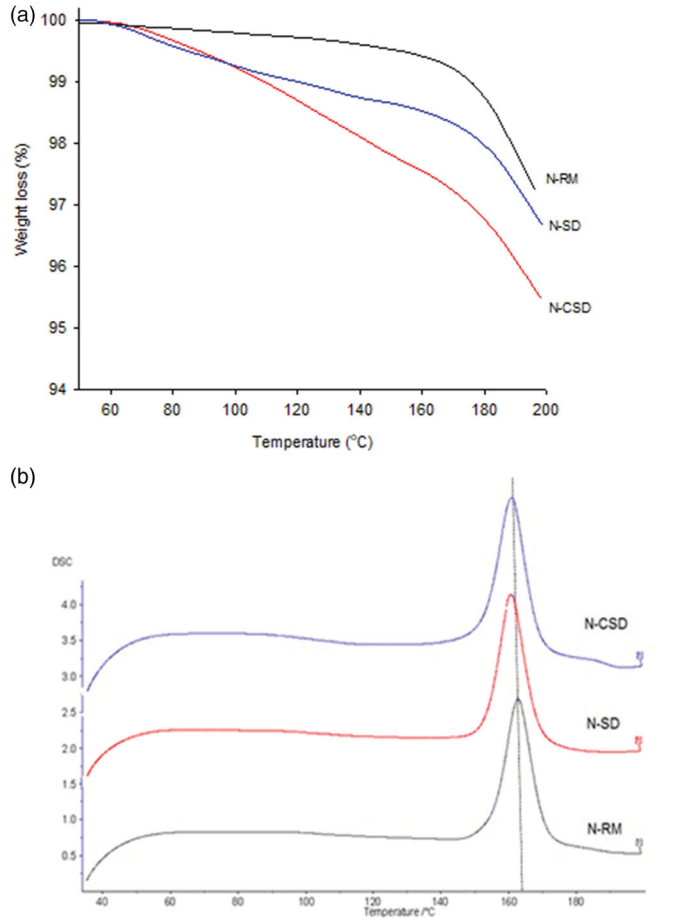


Figure 4. Thermogravimetric (a) and DSC analysis (b) for naproxen unprocessed (N-RM), spray-dried (N-SD) and co-spray dried (N-CSD).

structure and m.p. reduction compared to the pure drug (Paudel et al. 2010). The interaction is supported by the closeness of the values of the Hansen total solubility parameters of 22.2 $MPa^{0.5}$ for naproxen (Tsivintzelis et al. 2009, Table 4 in their paper) and 28.7 $MPa^{0.5}$ for HPMC (Archer 1992, Table 9 in his paper). Their difference of 6.5 $MPa^{0.5}$ indicates that they are likely to be miscible. The measured melting enthalpies of the three drug forms N-RM, N-SD and N-CSD were: 143.2, 122.2 and 100.5 μVs/mg. This is the same decreasing order as the m.p. and signifies that the liquid state is reached with less energy consumption due to loss of crystallinity caused by spray drying and drug-polymer interaction. In the case of co-spray dried drug, the lower enthalpy can also be attributed to drug dilution with HPMC.

### 3.3.2. Naproxen sodium

***TGA.*** In Figure 5, the TGA plots of weight loss with temperature are shown for the naproxen sodium forms. First derivatives of the TGA curves (dTGA) were plotted in order to clarify different drying steps. It can be seen that for the unprocessed (NS-RM) and spray dried drug alone (NS-SD) with water contents 2.9% and 2.8% (Table 2) the TGA curves decrease due to weight loss up to a temperature of about 130 °C, whereas for the co-spray dried form (NS-CSD) with higher water content (5.4%, Table 2) the decrease goes further up to about 150 °C. The weight changes are better seen in the corresponding superimposed dTGA curves. For NS-RM and NS-SD there is a slight water loss around 70 °C followed by a major one around 100 °C. On the other hand, for NS-CSD there are slight losses around 70 and 100 °C followed by a major at

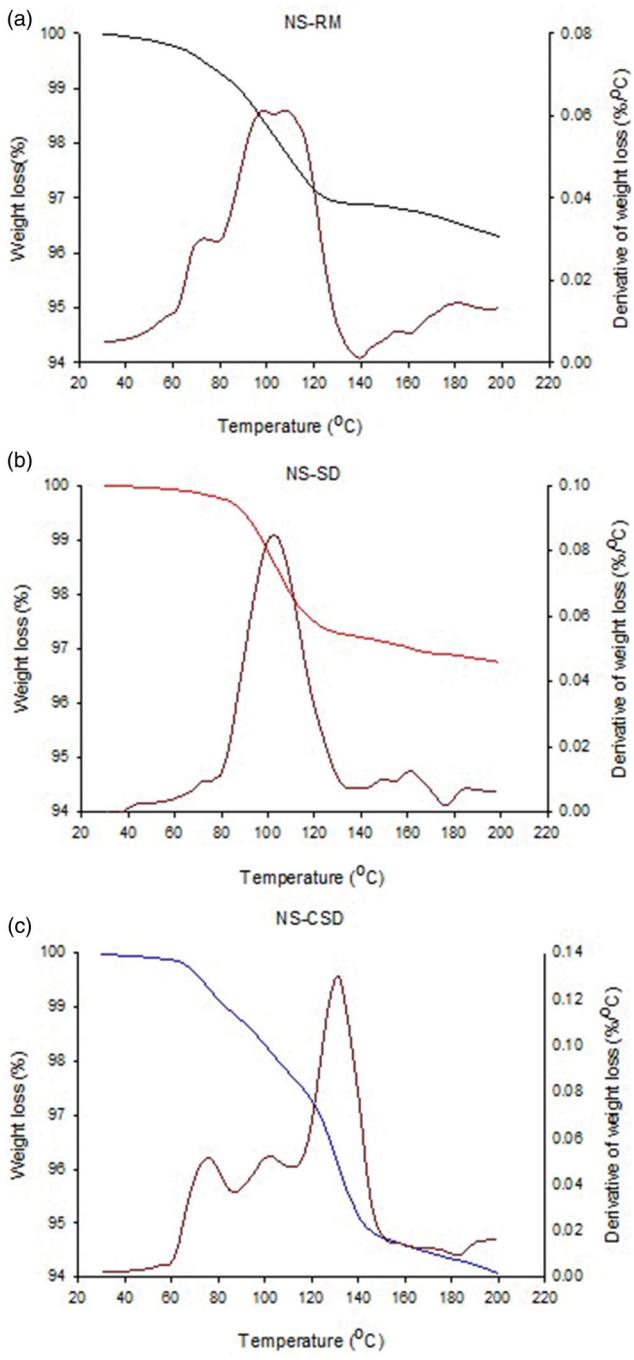


Figure 5. Thermogravimetric analysis recorded and derivatised curves for naproxen sodium unprocessed (a), spray-dried (b) and co-spray dried (c).

130 °C indicating presence of strongly bound hydrate water. The major water loss of NS-RM and NS-SD occurs at about 30 °C higher than the temperature reported for the loss of monohydrate water (about 70–80 °C) by Kim et al. (2005). This could be ascribed to the perforated sample holder used in this work instead of an open pan (Di Martino et al. 2008). The multistep pattern of water loss of NS-CSD is in agreement with the previously-reported multistep dehydration of dihydrate naproxen sodium (Di Martino et al. 2001). Furthermore, it has been reported that the presence of hygroscopic excipients delays dehydration of naproxen sodium due to their preferential drying over dehydration (Thakral et al. 2019). Therefore, the dehydration shift in the TGA curve of NS-CSD could be partly attributed to the presence of HPMC.

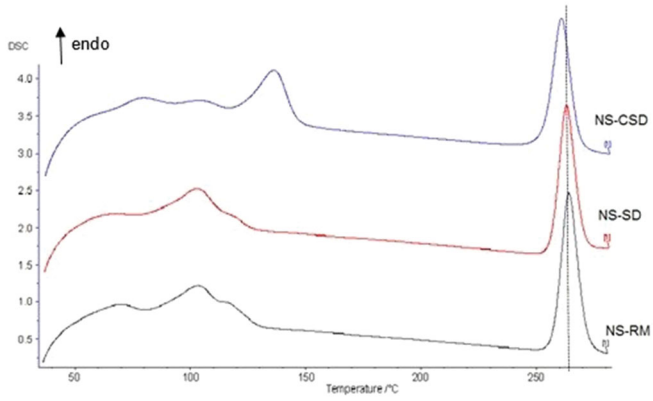


Figure 6. DSC thermograms for naproxen sodium (unprocessed NS-RM; spray-dried NS-SD; co-spray dried NS-CSD).

***DSC.*** From Figure 6, it can be seen that overall, the thermograms of naproxen sodium forms were more eventful than naproxen showing four endothermic peaks each. The main melting peaks occur at 264.4, 262.6 and 260.3 °C, with melting enthalpies 115.9, 105.5 and 99.0 μVs/mg for the unprocessed (NS-RM), spray-dried (NS-SD) and co-spray dried (NS-CSD) forms, respectively. The lower enthalpy by 16.9 μVs/mg of NS-CSD is partially attributed to the fact that it was calculated using the initial sample weight, which included water of hydration. The melting point (m.p.) depression by 4.1 °C of NS-CSD indicates lattice deformation, which may have been induced by the spray drying process in the presence of polymer (Al-Zoubi et al. 2017). Dehydration during thermal analysis may be another reason for lattice deformation (Li et al. 2000). Smaller and broad, not-well-separated endotherms are seen in the thermograms at temperatures below 150 °C indicating multistep dehydration.

For all three naproxen sodium forms a small not well-formed peak appears at about 70 °C corresponding to the small peak (first from the left) in the TGA curves (Figure 5). The second DSC peak seen of NS-RM, NS-SD (well defined) and NS-CSD (small and broad) appears at about 100 °C and corresponds to the second peak in the corresponding TGA curves. For NS-RM and NS-SD this DSC peak possibly represents dehydration of monohydrate naproxen sodium. The difference of 14 °C from the temperature of 86.0 °C reported by Kim and Rousseau (2004) can be explained by the use of open pan in their work, which facilitated dehydration compared to perforated pan (Di Martino et al. 2008). For NS-CSD the small peak at 100 °C should be attributed to the dehydration of HPMC as previously reported (Vueba et al., 2006). The third peak seen in the DSC of NS-CSD at about 125 °C corresponding to high water loss in the TGA plots (Figure 5(c)) should be attributed to dehydration of monohydrate. The shifting to higher temperatures compared to the reported temperature of 80–100 °C can be ascribed to the different type of pan holder and to the presence of the hydrophilic binder HPMC (Di Martino et al. 2001; Thakral et al. 2019).

### 3.4. Solid-state characterization

The different forms of naproxen and naproxen sodium before and after spray drying alone or with polymer were characterized for crystallinity changes by PXRD. Changes in the hydroxyl and carboxylic groups, in the aromatic rings and in the moiety connecting the isopropionic acid and the naphthalene structure were examined by vibration spectroscopy. The results of PXRD, FTIR and Raman analyses are presented in Figures 7–9.

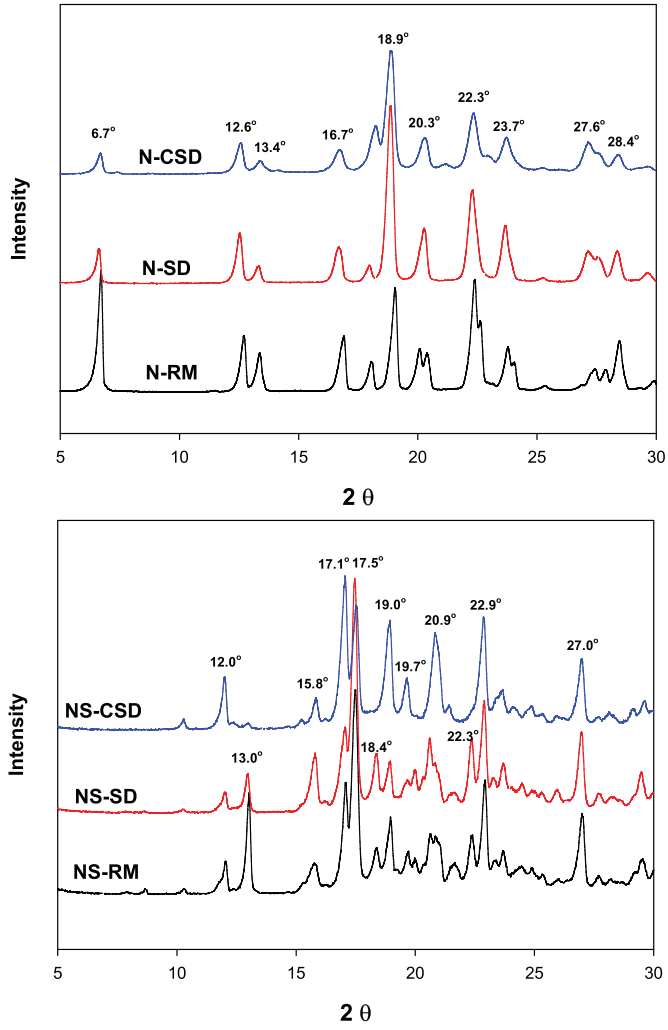


Figure 7. PXRD patterns for (a) naproxen (unprocessed N-RM; spray-dried N-SD; co-spray dried N-CSD) and (b) naproxen sodium (unprocessed NS-RM; spray-dried NS-SD; co-spray dried NS-CSD).

#### 3.4.1. Powder x-ray diffraction (PXRD)

The PXRD patterns of unprocessed naproxen and its salt (N-RM, NS-RM), naproxen and salt spray-dried alone (N-SD, NS-SD) and co-spray dried forms (N-CSD, NS-CSD) are shown in Figure 7(a). It is noticed that all diffraction patterns are composed of subsequent sharp reflections indicating crystalline structure. The PXRD pattern of N-RM show diffraction peaks characteristic of naproxen at 2$\theta$: 6.7, 12.6, 13.4, 16.7, 18.1, 19.1, 20.4, 22.3, 23.8, 27.2, 27.5, 28.4 degrees). These were also present in the spray-dried samples, suggesting that unprocessed and spray-dried powders belong to the same crystal lattice. However, there are differences in the relative intensities of the reflections, with most reflections in the patterns of N-CSD and N-SD having lower intensity compared to N-RM (i.e. at 2 $\theta = 6.7$, 12.6, 13.4, 16.7, 22.3 and 28.4 degrees). This is attributed to differences in the crystallinity (Jbilou et al. 1999). Furthermore, the effect of clear particle shape differences (Figure 3) cannot be excluded (Marshall and York 1989; El-Said 1995; Garekani et al. 1999; Nokhodchi et al. 2003) and may explain why few peaks appear with higher intensity in the spray-dried samples (at 2 $\theta = 18.9$ and 27.6 degrees).

It has been reported that for naproxen such crystalline to amorphous transformation is difficult due to the great recrystallization tendency associated with high m.p. drugs (Löbmann et al. 2011). Therefore, the present results suggest that certain degree

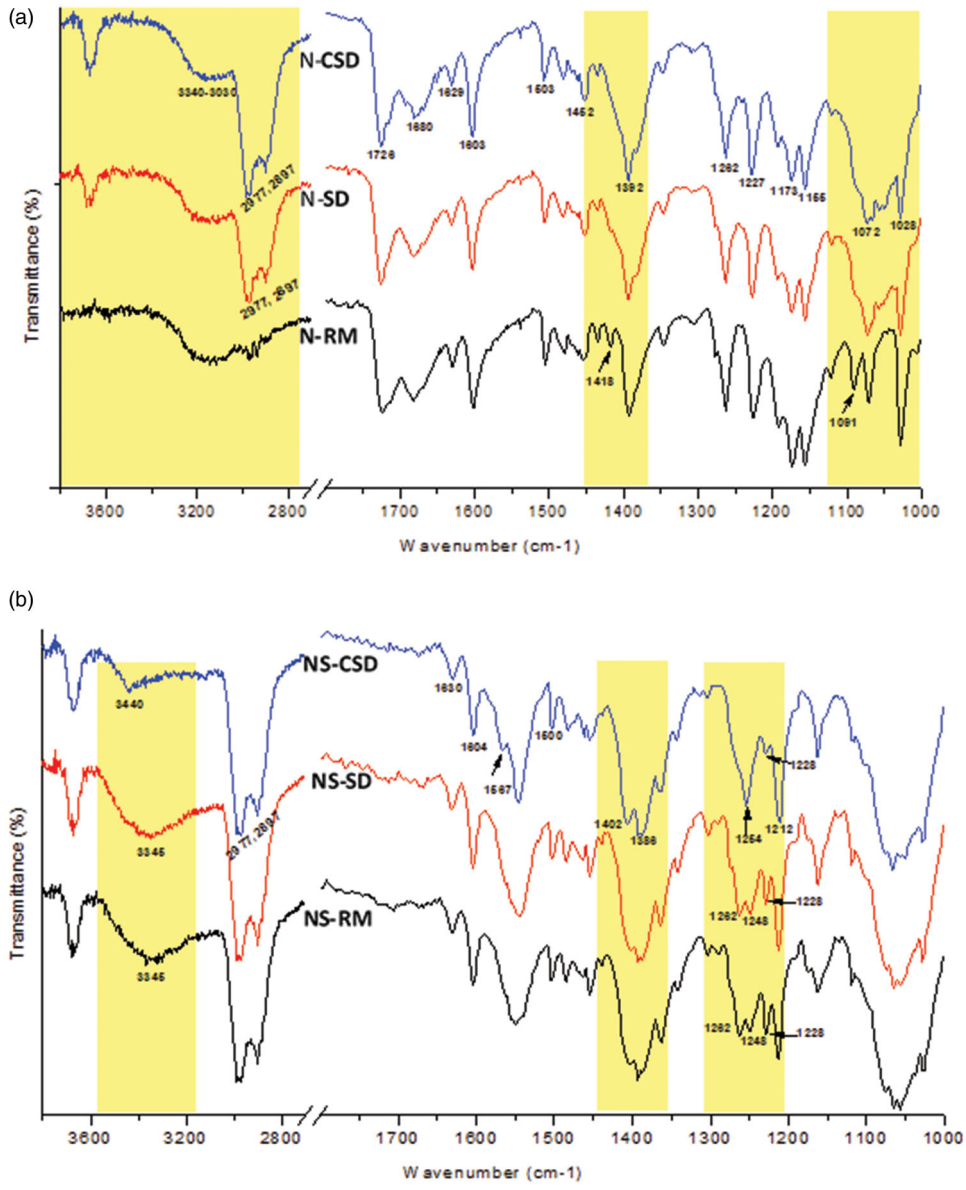


Figure 8. FTIR spectra for (a) naproxen (unprocessed N-RM; spray-dried N-SD; co-spray dried N-CSD) and (b) naproxen sodium (unprocessed NS-RM; spray-dried NS-SD; co-spray dried NS-CSD).

of crystallinity loss takes place during spray drying and it is stabilized by HPMC through interaction of its H-bonding –OH donor group with the carboxylic moiety of naproxen. This crystallinity loss may inflict changes in mechanical properties.

Considering the PXRDs of naproxen sodium (Figure 7(b)), they demonstrate similarities between NS-RM and NS-SD indicating that they have similar solid-state composition. However, the pattern of the co-spray dried form (NS-CSD) exhibits considerable discrepancies from the other two, suggesting a different pseudopolymorphic composition. In particular, the PXRD pattern of NS-CSD shows a reflection at $2\theta = 12°$, which is characteristic of the dihydrate form (Kim et al. 2005; Thakral et al. 2019) and a reflection at $2\theta = 17.1°$, which conforms with the pattern of the monohydrate form (Kim and Rousseau 2004; Malaj et al. 2009). On the other hand, the reflections at $2\theta = 12.0°$ and $17.1°$ in the PXRDs of NS-RM and NS-SD are much smaller, implying existence of dihydrate and monohydrate but in small proportions. Besides, the reflection in the PXRDs of NS-RM and NS-SD at $2\theta = 13.0°$ is characteristic of the anhydrate form.

Overall, the similarity of NS-RM and NS-SD PXRD patterns and the presence of characteristic diffraction lines of anhydrous form, are in agreement with the similarity of their DSC, TGA and dTGA thermograms and with their similar water content corresponding to a high proportion of anhydrous form and low proportions of monohydrate and dihydrate forms (Table 2). On the other hand, the presence of characteristic peaks of monohydrate and dihydrate in the PXRD pattern of NS-CSD is in agreement with the distinctive DSC, TGA and dTGA thermograms of this batch and with its higher water content (Table 2).

### 3.4.2. Vibration spectroscopy

*3.4.2.1. FTIR.* In Figure 8, FTIR spectra for naproxen and naproxen sodium unprocessed (N-RM and NS-RM), spray-dried (N-SD and NS-SD) and co-spray dried (N-CSD and NS-CSD) are presented. Characteristic bands are numbered principally in the spectrum of the co-spray dried drug. Arrows have been added to indicate the presence of extra bands or variations in band intensities.

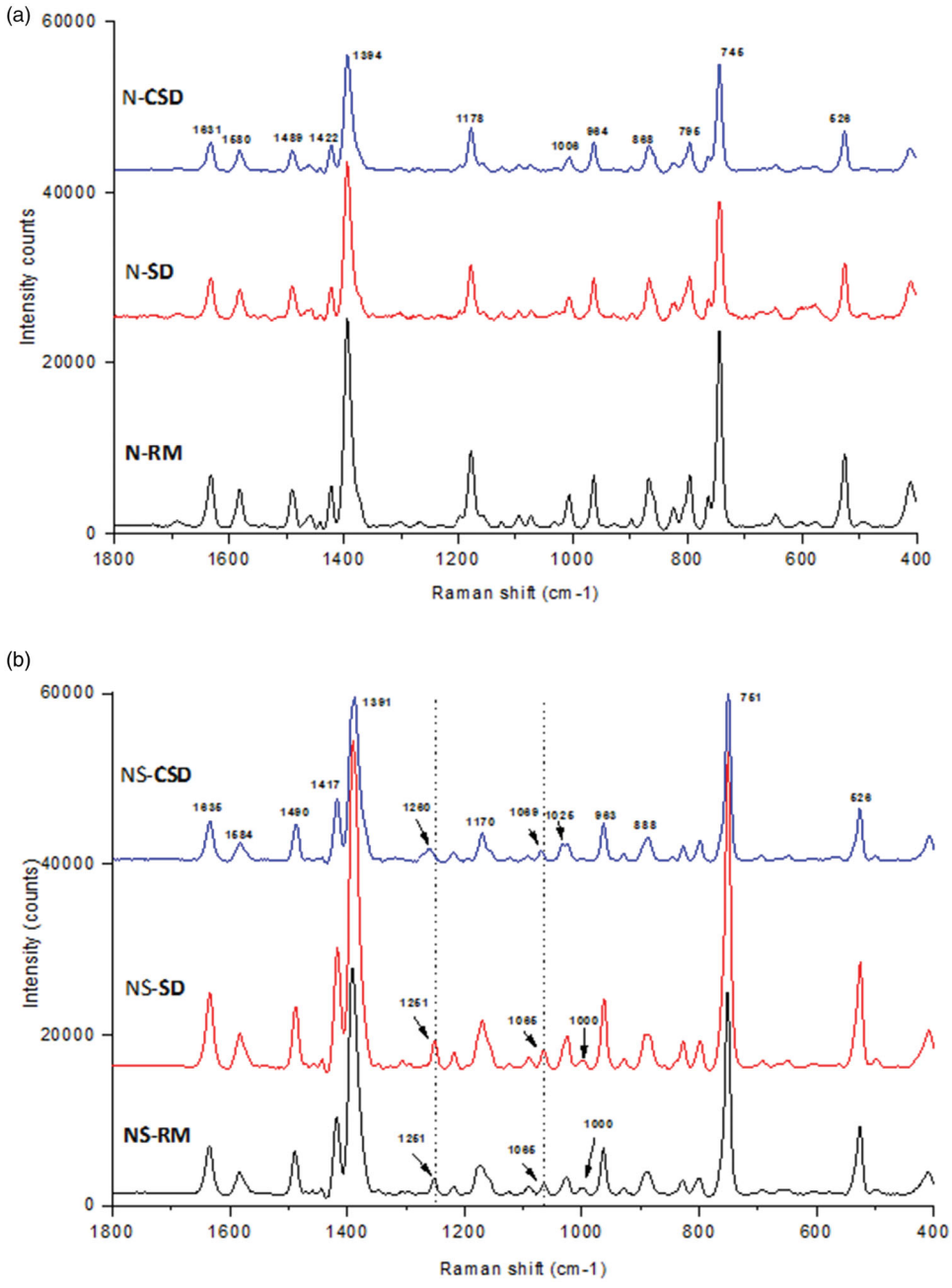


Figure 9. Raman spectra for (a) naproxen (unprocessed N-RM; spray-dried N-SD; co-spray dried N-CSD) and (b) naproxen sodium (unprocessed NS-RM; spray-dried NS-SD; co-spray dried NS-CSD).

*Naproxen*. In Figure 8(a), the broad band between 3340 and 3030 $cm^{-1}$ is due to stretching of the carboxylic acid –OH in the H-bonded dimer. Further bands are observed at 17 261 680 $cm^{-1}$ (asymmetric carbonyl stretching for the monomer and dimer respectively) (Paudel and Van Den Mooter 2012), 1629 and 1603 $cm^{-1}$ (C–C ring stretching and C–H ring bending), 1503 $cm^{-1}$ (asymmetric C–H in the carboxylic acid and ring stretching), and 14 521 392 $cm^{-1}$ (C–C ring stretching and C–H ring bending), 1262, 1227, 1173 and 1155, 1072 and 1028 $cm^{-1}$ (C–H ring bending and rocking) (Jubert et al. 2006).

It is noticed that some bands of the N-RM spectrum are absent or reduced in the spray-dried form, and vice versa. These changes could be related to loss of crystallinity due to spray drying. More specifically, the bands at 1091 $cm^{-1}$ (C–H rocking/bending vibration corresponding to the intermediate carbon in the propionic acid, which is connected to the naphthalene ring) and 1418 $cm^{-1}$ (C–C ring stretching and C–H ring bending) seen in the spectrum of N-RM are absent from the spray-dried forms. Furthermore, the intensity of band at 1028 $cm^{-1}$ is high in N-RM but reduced in the spray-dried forms. On the other hand, C–H stretch bands at 2977 and 2897 $cm^{-1}$ (Lin-Vien et al. 1991; Saji et al. 2020), which are pronounced in the spectra of N-SD and N-CSD are minute in the N-RM.

*Naproxen sodium*. In Figure 8(b), the spectra of the three forms are compared. An overall resemblance is noticed. Unlike naproxen (Figure 8(a)), the C–H bands at 2977 and 2897 $cm^{-1}$ are distinct in all three spectra of naproxen sodium. Further bands are observed at 1630 and 1604 $cm^{-1}$ (C–C stretching), 1545 $cm^{-1}$ (O–C stretching), 1500, 1481 and 1452 $cm^{-1}$ (C–C, H–C–H and H–C–C stretching) (Lin-Vien et al. 1991). The last bands at 1162 and 1065 $cm^{-1}$ seen in all spectra are due to H–C–C bending and C–C stretching/bending (Saji et al. 2020).

Table 3. Work of compaction (Wc), work of decompression (Wd), plastic/elastic energy ratio (EE/PE), slope of force/displacement derivative plot, maximum ejection force ($F_{ej}$) and tensile strength of the experimental powders (mean ± standard deviation, $n = 3$).

| | | | | | | Tensile strength (MPa) | |
|---|---|---|---|---|---|---|---|
| Batch code | Wc (J) | Wd (J) | EE/PE | Slope (mm) | $F_{ej}$ (N) | RH 40%, 20 °C | RH 75%, 40 °C |
| N-RM | 2.64 ± 0.173 | −0.63 ± 0.006 | 0.19 ± 0.011 | 0.59 ± 0.055 | 330 ± 57 | 2.09 ± 0.01 | 1.72 ± 0.16 |
| N-SD | 2.99 ± 0.015 | −0.59 ± 0.012 | 0.17 ± 0.003 | 0.68 ± 0.017 | 213 ± 33 | 3.85 ± 0.34 | 1.81 ± 0.74 |
| N-CSD | 3.12 ± 0.079 | −0.57 ± 0.006 | 0.15 ± 0.003 | 0.75 ± 0.010 | 142 ± 19 | 4.19 ± 0.90 | 2.03 ± 0.27 |
| NS-RM | 2.41 ± 0.075 | −0.55 ± 0.006 | 0.19 ± 0.006 | 0.47 ± 0.021 | 99 ± 18 | 1.91 ± 0.23 | 2.27 ± 0.17 |
| NS-SD | 2.74 ± 0.032 | −0.54 ± 0.006 | 0.16 ± 0.003 | 0.62 ± 0.021 | 73 ± 9 | 2.93 ± 0.55 | 2.42 ± 0.16 |
| NS-CSD | 2.86 ± 0.076 | −0.56 ± 0.006 | 0.16 ± 0.005 | 0.72 ± 0.017 | 107 ± 16 | 4.56 ± 1.01 | 3.62 ± 0.03 |

Nevertheless, besides their common bands, the spectra of the three naproxen sodium forms show distinct differences, which are related to their solid-state composition. The large band at 1545 $cm^{-1}$ in the NS-RM and NS-SD spectra is narrower in the NS-CSD with parallel formation of a shoulder band at 1567 $cm^{-1}$. The bands at 14 021 386 $cm^{-1}$ (C–C stretching) appear in all spectra, but they are better formed in the NS-CSD. Bands at 1262 and 1248 $cm^{-1}$ (H–C–C bending and C–C bending/stretching) in the spectra of NS-RM, NS-SD, are merged in the NS-CSD into a strong band at 1254 $cm^{-1}$. Additionally, the 1228 $cm^{-1}$ band (C–C stretching/bending) has much lower intensity in the co-spray dried form.

*3.4.2.2. Raman.* In Figure 9, spectra of the different forms of naproxen and its sodium salt are presented. In Figure 9(a), major naproxen bands were recorded at 1 631 158 014 891 420 $cm^{-1}$ (C–C ring stretching, C–H ring bending), 1394 $cm^{-1}$ (asymmetric C–C stretching), 1178 $cm^{-1}$ (asymmetric C–H vibration) 964 868 797 $cm^{-1}$ (C–H ring bending, C–H bending/rocking), 743 $cm^{-1}$ (ring stretching) and 526 $cm^{-1}$ (ring deformation and C–H rocking) (Saji et al. 2020). There are no noticeable differences in the band positions of the three forms.

On the other hand, the spectra of naproxen sodium (Figure 9(b)) show differences between the unprocessed (NS-RM), spray-dried (NS-CS) and co-spray dried (N-CSD) forms. In particular, the band at 1251 $cm^{-1}$ (H–C–C stretching) in NS-SD and NS-CSD has been shifted slightly to 1260 $cm^{-1}$ in the NS-CSD. Other subtler differences such as: shift of 1065 band to 1069 $cm^{-1}$ in the spectrum of NS-CSD, absence of band at 1000 $cm^{-1}$ in the NS-CSD and change of band shape at 1025 $cm^{-1}$ in the NS-CSD spectrum (Saji et al. 2020) are classified as minor, reflecting small changes in the molecular conformation.

Overall, the differences among the spectra of naproxen and among the spectra of naproxen sodium are more obvious in the FTIR analysis. They confirm solid-state alterations described in the PXRD patterns and indicate differences in molecular conformation that are expected to affect their mechanical properties.

### 3.5. Compaction behaviour

The compaction behaviour was studied by analysing force/displacement profiles. The work of compaction ($W_c$), work of decompression ($W_d$) (Figure 1) and the ratio of elastic/plastic energy (EE/PE) were computed and values are presented in Table 3 together with the maximum tablet ejection force ($F_{ej}$).

#### 3.5.1. Force-displacement profiles

From Table 3, it can be seen that for both spray-dried naproxen and its salt the trend of $W_c$ expressing the absorbed work is: co-spray dried > spray-dried alone > unprocessed neat powder, while for $W_d$ the trend is reversed. The increase of $W_c$ due to spray drying can be attributed to several reasons. The formation of amorphous regions as indicated by the PXRD, DSC and spectroscopic analysis may increase reactivity and surface deformability (Berggren et al. 2004; Al-Zoubi et al. 2017). Spray-dried particles, being agglomerates, are more porous than unprocessed powder and hence more compressible, thus increasing contact area (Sakhnini et al. 2015). The additional increase of $W_c$ in the co-spray dried powders is attributed to the multi-functionality of HPMC. It acts as a binder developing further interparticle bonding areas but also as a crystal growth inhibitor reducing crystallinity. Additionally, it delays dehydration during spray drying, leading to higher water content of dihydrate and monohydrate forms, and thus increasing their plasticity (Malaj et al. 2010). The decrease of $W_d$ should be related to the softer nature of spray-dried product and the greater strength of interparticle bonds in the presence of HPMC. The above changes of $W_c$ (increase) and decrease of $W_d$ (decrease) due to spray drying of the drugs alone or co-spray dried with HPMC resulted in an overall decrease of the ratio EE/EP representing the fraction of compaction energy that is expended as elastic deformation during decompression (Garr and Rubinstein 1991).

Furthermore, Table 3 presents values of the slope of derivatised compression curves, i.e. first derivative of punch displacement with respect to applied force (Gharaibeh and Aburub 2013). These plots are shown in Figure 10 and they are seen to be straight lines over 1–5 kN compression range ($R^2$ for: N-RM 0.953, N-SD 0.970, N-CSD 0.964, NS-RM 0.975, NS-SD 0.942 and NS-CSD 0.923). It has been suggested that materials with high slope values compact predominantly by plastic deformation, while materials with low slope values by fragmentation (Gharaibeh and Aburub 2013). From Table 3, it is seen that the values of the slopes ranged from 0.47 to 0.75 mm increasing in the order co-spray dried > spray-dried alone > unprocessed, indicating that co-spray drying leads to greater plasticity. From the above discussion, it is concluded that spray drying and in particular co-spray drying with HPMC produce particles with greater work of compaction and improved compressibility.

Furthermore, from Table 3 it can be seen that the maximum ejection force ($F_{ej}$) is lower for naproxen sodium than naproxen acid, which could be related to differences in particle shape and properties of the formed compact. Unprocessed naproxen (N-RM) exhibited remarkably high $F_{ej}$ (339 N), which could be explained by the increased adhesion and friction due to the flaky particle shape and high elastic recovery indicated by high $W_d$ value (0.63 J, Table 3). Although both naproxen and its salt spray dried alone exhibit reduced $F_{ej}$, the effect of co-spray drying on $F_{ej}$ was different. For N-CSD the $F_{ej}$ was less than for N-SD and N-RM, which can be attributed to increased compressibility and reduced elastic recovery. Conversely, for naproxen sodium $F_{ej}$ was higher for NS-CSD, probably due to its high-water content (5.4%, Table 2) imparting stickiness to the powder.

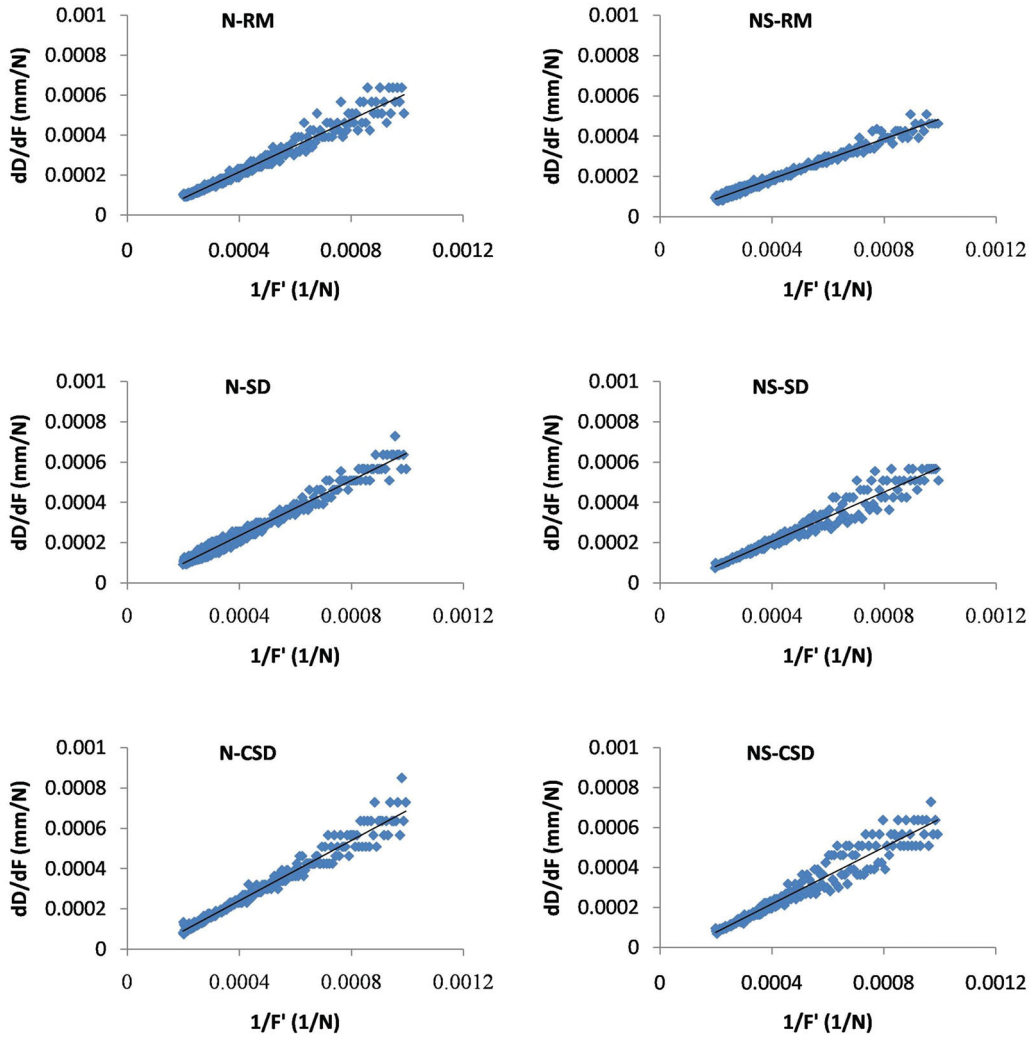


Figure 10. Representative first derivative of force-displacement plots of (dX/dF) vs 1/F′ for naproxen (N-RM, N-SD, N-CSD) and naproxen sodium (NS-RM, NS-SD, NS-CSD).

### 3.5.2. Tabletability and compactability

The tabletability and compactability plots of ready-to-compress (RTC) mixtures of naproxen and naproxen sodium (with crospovidone, sodium stearyl fumarate and talc) are presented in Figure 11.

Consider naproxen first (Figure 11(a)). It can be seen that in the compression range 72 and 295 MPa, N-SD RTC formed tablets with strength from 1.2 to 2.1 MPa, whereas N-CSD RTC formed stronger tablets with strength from 2.3 to 4.2 MPa. On the other hand, N-RM RTC mixtures failed to produce intact tablets when compressed under similar conditions. The ability of N-SD to form tablets should be attributed mainly to the more porous structure of the agglomerated N-SD particles (Figure 3) associated with fragmentation during compaction, increased interparticle contact and surface area. To a small extent, it may be attributed to amorphization and increased surface plasticity as indicated by the higher work of compaction ($W_c$), lower elastic/plastic energy (EE/PE) and lower slope of derivatised compression curve (Table 3). The remarkably higher compactability and tablet strength of the N-CSD RTC seen in Figure 11(a), is attributed partly to the significant modification of the crystal lattice (Figure 7(a)) but mainly to the high binding efficiency of HPMC signifying its importance in the formation of interparticle bonds between the co-spray dried particles. Application of higher compression pressures to N-SD or N-CSD RTC caused capping.

Next consider the compression of naproxen sodium (Figure 11(b)). All RTC powder mixtures of the three forms (NS-RM, NS-SD and NS-CSD) were compressible producing intact tablets of sufficient strength in the compression pressure range 72-443 MPa. From Figure 11(b) it is seen that the compactability and tensile strength of tablets from RTC mixtures of NS-RM and NS-SD are comparable, whereas the compactability and the strength of tablets of NS-CSD RTC mixtures demonstrated remarkably higher strength. As already mentioned, this is attributed to the high binding efficiency of HPMC and to the higher dihydrate content, which has been reported to be more compactable than the anhydrous drug (Malaj et al. 2010). It is interesting to notice in the tabletability plot of NS-CSD, that above a compression pressure of 140 MPa, the tablet strength decreases (Figure 10(b)). This may be explained by a change of the moisture state in the hydrated naproxen sodium particles, acting as plasticizer at low levels but being expelled to the particle surface, forming an aqueous layer which masks interparticle interactions and bond formation (Avgoustakis and Nixon 1993; Lamešić et al. 2017). To check the possibility of transformation of NS-CSD due to the applied pressure, FTIR spectra of tablets compressed at low (52 MPa) and high (174 MPa) pressures were compared with the spectrum of the NS-CSD uncompressed powder. These are shown in Figure 12 where it can be seen that the band at 3440 $cm^{-1}$ of the hydrate retained its position in the tablets at both low and high pressure

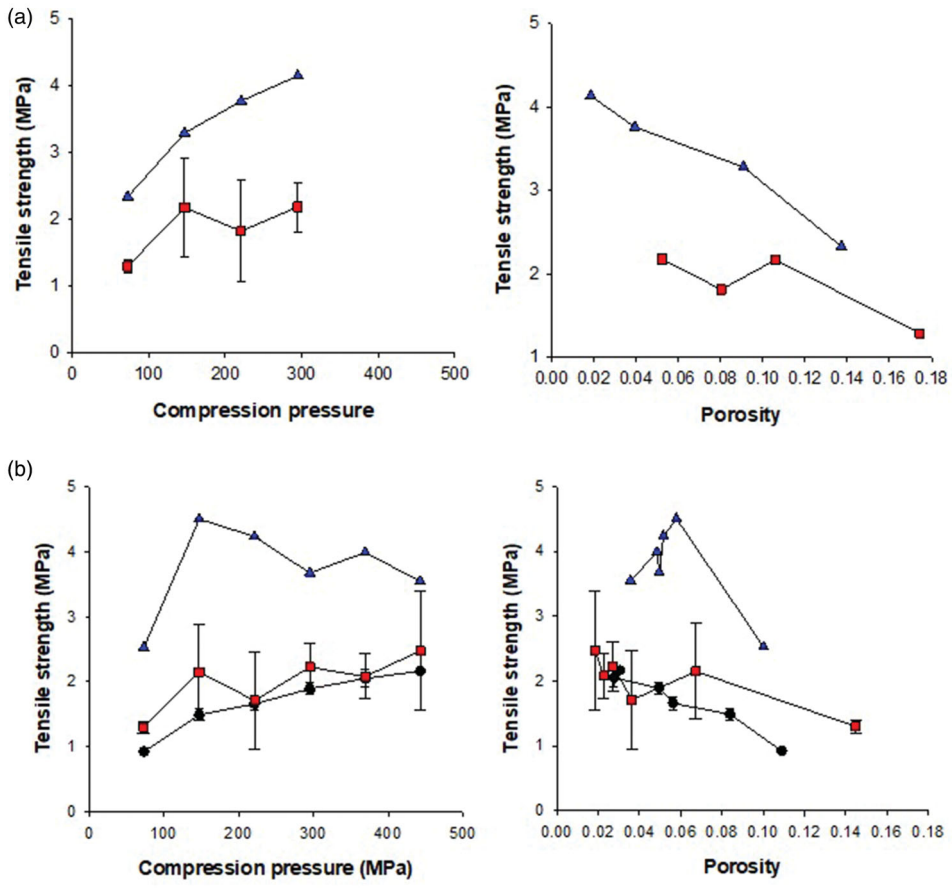


Figure 11. Tabletability (left) and compactability (right) plots of ready-to-compress mixtures of (a) naproxen and (b) naproxen sodium. Symbols in (a): squares N-SD, triangles N-CSD; symbols in (b): circles NS-RM, squares NS-SD, triangles NS-CSD). Error bars represent standard deviation ($n = 3$).

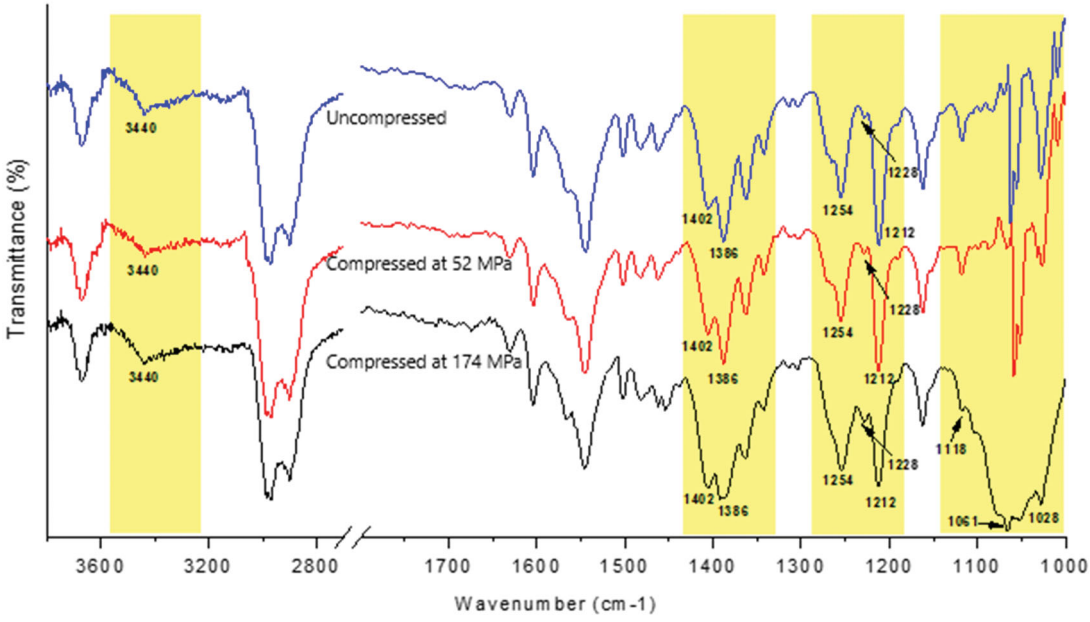


Figure 12. FTIR spectra of naproxen co-spray dried (NS-CSD) and corresponding tablets compressed at low (52 MPa) and high (174 MPa) pressure.

and did not shift to 3345 $cm^{-1}$ as in NS-RM and NS-SD forms (Figure 8(b)). Also, the band at 1254 $cm^{-1}$ remained single without changing to a double band as in NS-RM and NS-SD (Figure 8(b)). The sharper higher intensity bands of the tablets compared to corresponding powders seen in Figure 12 in the wavelength range 1150–1000 $cm^{-1}$ should be attributed to the high molecular density due to the close arrangement of the particles in the compressed tablet.

In Table 3 (last two columns on the right), results of accelerated test for tablet strength are presented. A decrease is seen in the strength of naproxen tablets, especially those from the spray-dried N-SD and N-CSD drug forms (~52–53%). This is ascribed to

moisture adsorbed by the tableting aid crospovidone, which is present in all drug forms and which at the test condition of 75% RH absorbs 20–25% moisture (Bühler 2008). Additionally, the existence of amorphous regions in the spray dried drug forms increases the moisture uptake resulting in greater strength reduction (Sheokand et al. 2014). The effect of moisture on tablet strength depends on its distribution and the physicochemical state (Malamataris et al. 1994). Strength reduction results from loosely bound moisture adsorbed by the hydrophilic polymers and the amorphous drug regions resulting in softening of the surfaces and masking of interparticle bonds. On the other hand, from Table 3 it is seen that exposure of naproxen sodium tablets to 75% RH increased the strength of neat drug tablets slightly but decreased the strength of the processed NS-SD and NS-CSD drug tablets. The reduction of NS-SD and NS-CSD tablets is quite smaller than that of naproxen spray dried N-SD and N-CSD (i.e. ~17–22% compared with ~52–53%). This could be attributed to sodium ion in the naproxen salt which may retain some adsorbed moisture, and thus reduce the loosely adsorbed moisture which interferes with the bonding. Overall, the reduction even after exposure to harsh environmental conditions the tablets still retain sufficient strength (>1.72 MPa)

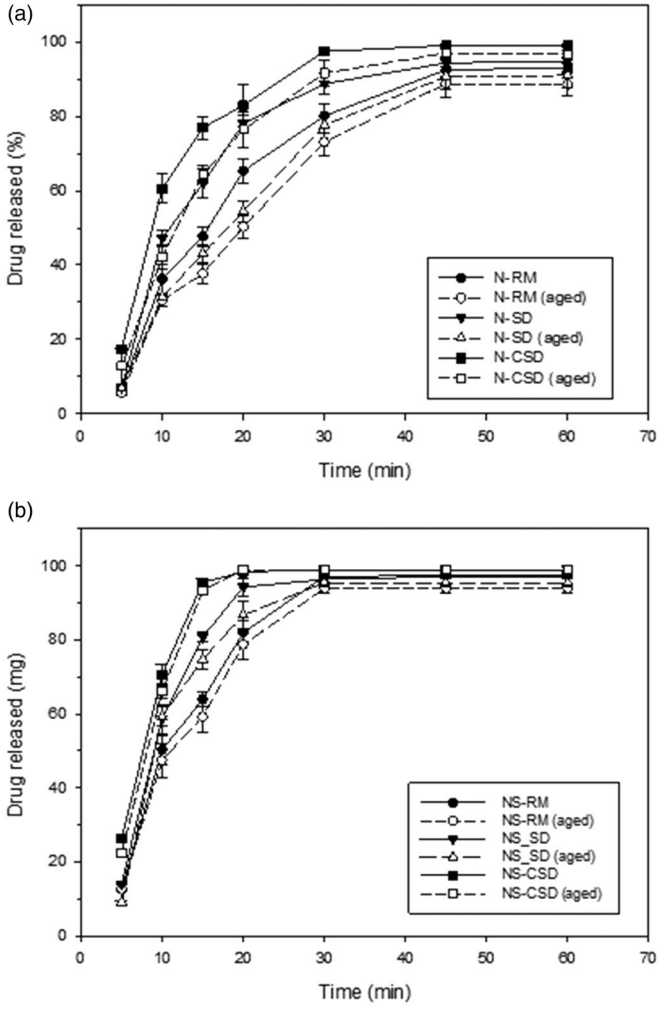


Figure 13. Drug released (%) (±SD, $n = 3$) from tablets of naproxen (a) and naproxen sodium (b) in simulated intestinal fluid (SIF).

### 3.6. In vitro *dissolution tests*

In Figure 13, dissolution profiles of naproxen and naproxen sodium are depicted as solid lines, whereas in Table 4 values of similarity factor ($f_2$) are given, comparing the entire dissolution profiles of tablets prepared from processed drugs with tablets from unprocessed drugs. Additionally, %drug released after 15 min values are given in Table 4 to compare the 'instant' release performance.

From the location of the curves in Figure 13 (circles for unprocessed, triangles for spray-dried drug alone and squares for co-spray dried) it appears that dissolution was completed after 60 min for naproxen tablets and after 30 min for naproxen sodium tablets. Spray drying improved considerably the dissolution rate of the tablets in the order: unprocessed drug < spray-dried alone < co-spray dried. This is confirmed by the released % drug data after 15 min test presented in Table 4. For naproxen these are: 47.61% for unprocessed (N-RM), 61.9% for spray-dried alone (N-SD) and 76.9% for co-spray dried (N-CSD) drug tablets; for naproxen sodium: 63.9% for unprocessed (NS-RM), 80.8% for spray-dried alone (NS-SD) and 95.5% for co-spray dried (NS-CSD) drug tablets, with the latter exceeding well the 85% threshold below which bioavailability may become dissolution limited (FDA 1997). Additionally, there are significant differences between the overall dissolution profiles of unprocessed and spray-dried drug tablets, as indicated by the low $f_2$ values of 52.17 for N-SD and 38.27 for N-CSD compared to N-RM tablets, and by the $f_2$ values of 51.7 for NS-SD and 38.76 for NS-CSD compared to NS-RM tablets. Such low $f_2$ values near or less than 50 indicate dissimilarity (Al-Zoubi et al. 2019).

Furthermore, in Figure 13 dissolution profiles of aged tablets (empty symbols/broken lines) are presented. Compared to green tablets (solid symbols/solid lines) the curves of the corresponding aged are shifted to the right, exhibiting slower release. This is more visible for naproxen and less for naproxen sodium. In the plateau curve regions, the differences in released drug are diminished. From the $f_2$ values given in Table 4 (last column, right), it appears that aging affected the release of all naproxen forms tablets, demonstrating low $f_2$ values of: 54.86 for N-RM, 52.65 for N-SD and 51.79 for N-CSD tablets which, however, are still above 50 which is the dissimilarity threshold. Conversely, the $f_2$ values for the tablets of naproxen sodium were high: 73.73 for N-RM, 69.20 for N-SD and 82.31 for NS-CSD tablets, signifying that there is no

Table 4. Drug release after 15 min testing and similarity factor ($f_2$) values comparing dissolution profiles of tablets of spray dried processed and co-processed tablets with those of unprocessed drugs (mean ± SD, $n = 3$).

| Batch code | %Released at 15 min | $f_2$ of processed tablets compared to tablets of neat drug | %Released at 15 min after aging | $f_2$ of aged tablets compared to green |
|---|---|---|---|---|
| N-RM | 47.6 ± 2.4 | – | 37.6 ± 2.4 | 54.86 |
| N-SD | 61.9 ± 3.2 | 52.17 | 43.1 ± 2.3 | 52.65 |
| N-CSD | 76.9 ± 3.0 | 38.27 | 64.2 ± 2.3 | 51.79 |
| NS-RM | 63.9 ± 1.8 | – | 59.3 ± 3.8 | 73.73 |
| NS-SD | 80.8 ± 1.2 | 51.71 | 74.8 ± 2.5 | 69.20 |
| NS-CSD | 95.5 ± 1.0 | 38.76 | 93.5 ± 1.1 | 82.31 |

dissimilarity between the dissolution profiles of green and aged tablets or that the tablets of naproxen sodium were less affected by the elevated humidity and temperature. Therefore, no physicochemical instability is anticipated under normal handling of naproxen and naproxen sodium tablets medication.

The improvement of release seen for the tablets of the spray-dried naproxen can be attributed to the effects of spray drying via reducing particle size and crystallinity, and to the presence of HPMC acting as a stabilizer of the disordered regions formed. These non-crystalline disordered regions of higher solubility promote faster drug release. Additionally, HPMC is expected to assist dissolution by facilitating wetting of the tablets due to its hydrophilic nature. In the case of naproxen sodium, spray-drying resulted in lower particle size, and presence of HPMC promoted higher content of the dihydrate form which has higher dissolution rate than the anhydrous (Di Martino et al. 2001).

## 4. Conclusions

The results of the present work demonstrate the feasibility of engineering naproxen and naproxen sodium particles by spray drying. The improved solid-state, micromeritic and mechanical properties of the engineered particles resulted in improved tabletability and dissolution. Enhancement was more pronounced when the drugs were co-processed with HPMC, enabling high drug loading (88% drug, 5% HPMC and 7% process aids) and adequate tensile strength (4 MPa) at the same time. Besides the binder action of HPMC, the mechanical improvement of the co-spray dried products is associated with the reduced crystallinity of naproxen and with the higher hydrate content of naproxen sodium during spray drying, as confirmed by PXRD, thermal analysis and vibration spectroscopy. Accelerated stability test (75% RH/40 °C) showed a minor effect on the release and mechanical strength of naproxen sodium and a greater effect for naproxen tablets, although not significant in terms of similarity dissolution index $f_2$.

## Disclosure statement

No potential conflict of interest was reported by the author(s).

## Funding

This research work received financial support from the Research Council, The Hashemite University, Zarqa–Jordan.

## References

Al-Zoubi N, Al-Obaidi G, Tashtoush B, Malamataris S. 2016. Sustained release of diltiazem HCl tableted after co-spray drying and physical mixing with PVAc and PVP. Drug Dev Ind Pharm. 42:270–279.

Al-Zoubi N, Odeh F, Nikolakakis I. 2017. Co-spray drying of metformin hydrochloride with polymers to improve compaction behavior. Powder Technol. 307:163–174.

Al-Zoubi N, Al-Rusasi A, Sallam AS. 2019. Ethanol effect on acid resistance of selected enteric polymers. Pharm Dev Technol. 24:24–34.

Angiolillo DJ, Weisman SM. 2017. Clinical pharmacology and cardiovascular safety of naproxen. Am J Cardiovasc Drugs. 17:97–107.

Archer WL. 1992. Hansen solubility parameters for selected cellulose ether derivatives and their use in the pharmaceutical industry. Drug Dev Ind Pharm. 18:599–616.

Arici M, Topbas O, Karavana SY, Ertan G, Sariisik M, Ozturk C. 2014. Preparation of naproxen-ethyl cellulose microparticles by spray-drying technique and their application to textile materials. J Microencapsul. 31:654–666.

Avgoustakis K, Nixon JR. 1993. Biodegradable controlled release tablets: II. preparation and properties of poly(lactide-co-glycolide) powders. Int J Pharm. 99:239–246.

Barot B, Parejiya P, Patel T, Parikh R, Gohel M. 2010. Development of directly compressible metformin hydrochloride by the spray-drying technique. Acta Pharm. 60:165–175.

Berggren J, Frenning G, Alderborn G. 2004. Compression behaviour and tablet-forming ability of spray-dried amorphous composite particles. Eur J Pharm Sci. 22:191–200.

Bhise KS, Dhumal RS, Paradkar AR, Kadam SS. 2008. Effect of drying methods on swelling, erosion and drug release from chitosan–naproxen sodium complexes. AAPS Pharm Sci Tech. 9:1–12.

British Pharmacopoeia Commission. 2020. British Pharmacopoeia Edition.

Bühler V. 2008. Kollidon: polyvinylpyrrolidone excipients for the pharmaceutical industry. 9th ed. Ludwigshafen (Germany): BASF SE.

Censi R, Rascioni R, Di Martino P. 2015. Changes in the solid state of anhydrous and hydrated forms of sodium naproxen under different grinding and environmental conditions: evidence of the formation of new hydrated forms. Eur J Pharm Biopharm. 92:192–203.

Di Martino P, Barthélémy C, Palmieri GF, Martelli S. 2001. Physical characterization of naproxen sodium hydrate and anhydrate forms. Eur J Pharm Sci. 14:293–300.

Di Martino P, Malaj L, Censi R, Martelli S. 2008. Physico-chemical and technological properties of sodium naproxen granules prepared in a high-shear mixer-granulator. J Pharm Sci. 97:5263–5273.

Di Martino P, Scoppa M, Joiris E, Palmieri GF, Andres C, Pourcelot Y, Martelli S. 2001. The spray drying of acetazolamide as method to modify crystal properties and to improve compression behaviour. Int J Pharm. 213:209–221.

El-Said Y. 1995. Effect of co-solvents on water content and physical properties of acetaminophen crystallized from aqueous solutions. STP Pharma Sci. 5:232–237.

FDA. 1997. Guidance for industry: dissolution testing of immediate release solid oral dosage forms. Rockville (MD): Center for drug evaluation and research.

Garekani HA, Ford JL, Rubinstein MH, Rajabi-Siahboomi AR. 2001. Effect of compression force, compression speed, and particle size on the compression properties of paracetamol. Drug Dev Ind Pharm. 27:935–942.

Garekani HA, Ford JL, Rubinstein MH, Rajabi-Siahboomi AR. 1999. Formation and compression characteristics of prismatic polyhedral and thin plate-like crystals of paracetamol. Int J Pharm. 187:77–89.

Garr J, Rubinstein M. 1991. An investigation into the capping of paracetamol at increasing speeds of compression. Int J Pharm. 72:117–122.

Gharaibeh SF, Aburub A. 2013. Use of first derivative of displacement vs. force profiles to determine deformation behavior of compressed powders. AAPS PharmSciTech. 14:398–401.

Gonnissen Y, Remon JP, Vervaet C. 2007. Development of directly compressible powders via co-spray drying. Eur J Pharm Biopharm. 67:220–226.

Gonnissen Y, Verhoeven E, Peeters E, Remon JP, Vervaet C. 2008. Coprocessing via spray drying as a formulation platform to improve the compactability of various drugs. Eur J Pharm Biopharm. 69:320–334.

Jbilou M, Ettabia A, Guyot-Hermann AM, Guyot JC. 1999. Ibuprofen agglomerates preparation by phase separation. Drug Dev Ind Pharm. 25:297–305.

Joiris E, Di Martino P, Malaj L, Censi R, Barthélémy C, Odou P. 2008. Influence of crystal hydration on the mechanical properties of sodium naproxen. Eur J Pharm Biopharm. 70:345–356.

Joshi AB, Patel S, Kaushal AM, Bansal AK. 2010. Compaction studies of alternate solid forms of celecoxib. Adv Powder Technol. 21:452–460.

Jubert A, Legarto ML, Massa NE, Tévez LL, Okulik NB. 2006. Vibrational and theoretical studies of non-steroidal anti-inflammatory drugs ibuprofen [2-(4-isobutylphenyl)propionic acid]; naproxen [6-methoxy-α-methyl-2-naphthalene acetic acid] and tolmetin acids [1-methyl-5-(4-methylbenzoyl)-1H-pyrrole-2-acetic acid]. J Mol Struct. 783:34–51.

Kim YS, Paskow HC, Rousseau RW. 2005. Propagation of solid-state transformations by dehydration and stabilization of pseudopolymorphic crystals of sodium naproxen. Cryst Growth Des. 5: 1623–1632.

Kim YS, Rousseau RW. 2004. Characterization and solid-state transformations of the pseudopolymorphic forms of sodium naproxen. Cryst Growth Des. 4:1211–1216.

Lamešić D, Planinšek O, Lavrič Z, Ilić I. 2017. Spherical agglomerates of lactose with enhanced mechanical properties. Int J Pharm. 516:247–257.

Li Y, Han J, Zhang GGZ, Grant DJW, Suryanarayanan R. 2000. In situ dehydration of carbamazepine dihydrate: a novel technique to prepare amorphous anhydrous carbamazepine. Pharm Dev Technol. 5:257–266.

Lin-Vien D, Colthup NB, Fateley WG, Grasselli JG. 1991. The handbook of infrared and Raman characteristic frequencies of organic molecules. San Diego (CA): Academic Press.

Löbmann K, Laitinen R, Grohganz H, Gordon KC, Strachan C, Rades T. 2011. Coamorphous drug systems: enhanced physical stability and dissolution rate of indomethacin and naproxen. Mol Pharm. 8:1919–1928.

Maghsoodi M, Hassan-Zadeh D, Barzegar-Jalali M, Nokhodchi A, Martin G. 2007. Improved compaction and packing properties of naproxen agglomerated crystals obtained by spherical crystallization technique. Drug Dev Ind Pharm. 33:1216–1224.

Maghsoodi M, Taghizadeh O, Martin GP, Nokhodchi A. 2008. Particle design of naproxen-disintegrant agglomerates for direct compression by a crystallo-co-agglomeration technique. Int J Pharm. 351:45–54.

Maheri-Esfanjani H, Adibkia K, Barzegar-Jalali M, Javadzadeh Y, Mohammadi G. 2012. Preparation and evaluation of naproxen solid dispersions using spray drying method. Res Pharm Sci. 7: 367.

Malaj L, Censi R, Di Martino P. 2009. Mechanisms for dehydration of three sodium naproxen hydrates. Cryst Growth Des. 9: 2128–2136.

Malaj L, Censi R, Gashi Z, Di Martino P. 2010. Compression behaviour of anhydrous and hydrate forms of sodium naproxen. Int J Pharm. 390:142–149.

Malamataris S, Karidas T, Goidas P. 1994. Effect of particle size and sorbed moisture on the compression behaviour of some hydroxypropyl methylcellulose (HPMC) polymers. Int J Pharm. 103:205–215.

Marshall PV, York P. 1989. Crystallisation solvent induced solid-state and particulate modifications of nitrofurantoin. Int J Pharm. 55:257–263.

Mohammadzade M, Barzegar-Jalali M, Jouyban A. 2015. Solubility of naproxen in 2-propanol + water mixtures at various temperatures. J Mol Liq. 206:110–113.

Morris KR. 1999. Structural aspects of hydrates and solvates. In: Brittain HG, editor. Polymorphism in pharmaceutical solids. New York (NY): Marcel Dekker; p. 125–181.

Nikolakakis I, Pilpel N. 1985. Effect of particle shape on the tensile strengths of powders. Powder Technol. 42:279–283.

Nokhodchi A, Bolourtchian N, Dinarvand R. 2003. Crystal modification of phenytoin using different solvents and crystallization conditions. Int J Pharm. 250:85–97.

Paluch KJ, Tajber L, Adamczyk B, Corrigan OI, Healy AM. 2012. A novel approach to crystallisation of nanodispersible microparticles by spray drying for improved tabletability. Int J Pharm. 436:873–876.

Paluch KJ, Tajber L, Corrigan OI, Healy AM. 2013. Impact of alternative solid state forms and specific surface area of high-dose, hydrophilic active pharmaceutical ingredients on tabletability. Mol Pharm. 10:3628–3639.

Paudel A, Loyson Y, Van den Mooter G. 2013. An investigation into the effect of spray drying temperature and atomizing conditions on miscibility, physical stability, and performance of naproxen-PVP K 25 solid dispersions. J Pharm Sci. 102: 1249–1267.

Paudel A, Van Den Mooter G. 2012. Influence of solvent composition on the miscibility and physical stability of naproxen/PVP K 25 solid dispersions prepared by cosolvent spray-drying. Pharm Res. 29:251–270.

Paudel A, Van Humbeeck J, Van den Mooter G. 2010. Theoretical and experimental investigation on the solid solubility and miscibility of naproxen in poly(vinylpyrrolidone). Mol Pharm. 7: 1133–1148.

Rathod P, Mori D, Parmar R, Soniwala M, Chavda J. 2019. Co-processing of cefuroxime axetil by spray drying technique for improving compressibility and flow property. Drug Dev Ind Pharm. 45:767–774.

Saji RS, Prasana JC, Muthu S, George J, Kuruvilla TK, Raajaraman BR. 2020. Spectroscopic and quantum computational study on naproxen sodium. Spectrochim Acta A Mol Biomol Spectrosc. 226:117614.

Sakhnini N, Al-Zoubi N, Al-Obaidi GH, Ardakani A. 2015. Sustained release matrix tablets prepared from cospray dried mixtures with starch hydrophobic esters. Pharmazie. 70:177–182.

Sanoufi MR, Aljaberi A, Hamdan I, Al-Zoubi N. 2020. The use of design of experiments to develop hot melt extrudates for extended release of diclofenac sodium. Pharm Dev Technol. 25: 187–196.

Sheokand S, Modi SR, Bansal AK. 2014. Dynamic vapor sorption as a tool for characterization and quantification of amorphous content in predominantly crystalline materials. J Pharm Sci. 103: 3364–3376.

Stubberud L. 1995. Water-solid interactions: I. A technique for studying moisture sorption/desorption. Int. J. Pharm. 114:55–64.

Thakral S, Garcia-Barriocanal J, Thakral NK. 2019. Effect of processing conditions and excipients on dehydration kinetics of sodium naproxen hydrate in formulation. Int J Pharm. 557: 221–228.

Tsivintzelis I, Economou IG, Kontogeorgis GM. 2009. Modeling the phase behavior in mixtures of pharmaceuticals with liquid or supercritical solvents. J Phys Chem B. 113:6446–6458.

Vueba ML, Batista De Carvalho L, Veiga F, Sousa JJ, Pina ME. 2006. Influence of cellulose ether mixtures on ibuprofen release: MC25, HPC and HPMC K100M. Pharm Dev Technol. 11:213–228.

Worku ZA, Aarts J, Singh A, Van Den Mooter G. 2014. Drug-polymer miscibility across a spray dryer: a case study of naproxen and miconazole solid dispersions. Mol Pharm. 11:1094–1101.